Article

Journal of Intelligent Material Systems and Structures

Journal of Intelligent Material Systems and Structures
24(10) 1278–1285

DOI: 10.1177/1045389X12473377
jim.sagepub.com
SAGE

Effect of the piezoelectric hysteretic behavior on the vibration-based energy harvesting

Luciana L Silva[1], Marcelo A Savi[2], Paulo C Monteiro Jr[1] and Theodoro A Netto[1]

Abstract

Vibration-based energy harvesting has received great attention over the last years. The evaluation of the power output of the energy harvesters for different excitation frequencies and amplitudes of vibration has an important role in the design of the devices. In this regard, a wide range of nonlinear effects is observed having considerable influence on the generated power. The main goal of this contribution is to investigate the effect of the piezoelectric hysteretic behavior on the vibration-based energy harvesters. An archetypal model is employed to this aim by considering a one-degree-of-freedom mechanical system coupled to an electrical circuit by a piezoelectric element. Different hysteretic behaviors are investigated by considering the Bouc–Wen model. Numerical simulations are carried out establishing a comparison among hysteretic, nonlinear, and linear piezoelectric behaviors showing their influence on system dynamics.

Keywords

Energy harvesting, vibration, piezoelectricity, nonlinear dynamics, hysteretic behavior

Introduction

Smart materials have adaptive characteristics presenting a coupling between different fields such as mechanical, electrical, magnetic, and temperature. Specifically, piezoelectric materials have an electromechanical coupling presenting direct and inverse effects. Among the most important applications of piezoelectricity, the following should be highlighted: active vibration control, precision shape control, damage detection, and structural health monitoring (Crawley and de Luis, 1987; Hu and Ng, 2005).

Vibration-based energy harvesting is another promising use of the piezoelectric materials (Erturk and Inman, 2011; Liao et al., 2001). Energy harvesting has an increasing importance nowadays being the objective of several research efforts (Roundy et al., 2004). Mechanical vibration energy can be converted into electrical energy through piezoelectric elements used for power harvesting in various forms of structure (Sodano et al., 2004). As a result, electrical power can be stored or used to directly run and maintain low-power devices.

In recent years, there are several theoretical and experimental studies that investigate the design and performance optimization of vibration-based energy harvesters (duToit and Wardle, 2006; Erturk and Inman, 2008; Roundy et al., 2004; Sodano et al., 2004; Triplett and Quinn, 2009). In order to estimate the amount of power output of energy harvesting devices, several mathematical models have been developed to describe electromechanical coupling mechanisms. In this regard, the description of the piezoelectric electromechanical behavior points to a nonlinear constitutive behavior with hysteretic characteristics. Nevertheless, it is usual to adopt a linear relation between strain and electrical field. Under this assumption, there is a single constant for all values of strain–electrical field, known as the coupling coefficient.

The linear description of the piezoelectric materials can provide inconsistencies in the power output prediction of the energy harvester, as shown in Kim et al. (2010). duToit and Wardle (2006) showed that the use of linear constitutive relations underpredicted the

[1]COPPE—Department of Ocean Engineering, Universidade Federal do Rio de Janeiro, Rio de Janeiro, RJ, Brazil
[2]COPPE—Department of Mechanical Engineering, Universidade Federal do Rio de Janeiro, Rio de Janeiro, RJ, Brazil

Corresponding author:
Marcelo A Savi, COPPE—Department of Mechanical Engineering, Universidade Federal do Rio de Janeiro, P.O. Box 68503, Rio de Janeiro, 21941972, RJ, Brazil.
Email: savi@ufrj.br

experimental voltage produced from energy harvesting devices. Nonlinear effects have been identified in several situations. Crawley and Anderson (1990) presented experimental results by considering nonlinear behavior of the strain–electrical field, providing the evidence that a linear model is not valid for large strains. Triplett and Quinn (2009) treated a dynamical system with nonlinear stiffness considering nonlinear piezoelectric constitutive relation. The analysis of the power generated by the harvesting system suggests that nonlinear effects have considerable influence on the results and coincides with the inconsistencies in predicting the amount of power generated from the harvesting systems found in previous researches (duToit and Wardle, 2006).

This contribution deals with the vibration-based energy harvesting investigating hysteretic behavior of the piezoelectric element. An archetypal system composed by a one-degree-of-freedom mechanical system connected to an electrical circuit by a piezoelectric element is adopted. A discussion on the constitutive modeling of the piezoelectric materials is presented, using the Bouc–Wen model to describe hysteretic behavior. The main goal of this contribution is to investigate the effect of the hysteretic behavior on energy harvesting. Therefore, different hysteretic curves are investigated, and results are compared with those obtained with nonlinear and linear piezoelectric behaviors showing the influence of the hysteresis on system dynamics.

Vibration-based energy harvesting

An archetypal model to describe the vibration-based energy harvesting system is shown in Figure 1. It consists of a mechanical system connected to an electrical circuit by a piezoelectric element, responsible for the electromechanical conversion. A mass–spring–damper oscillator, with mass m, stiffness k, and a linear viscous coefficient b, represents the mechanical system. This system is subjected to a base excitation $u = u(t)$; the mass displacement is represented by y and z is the mass displacement relative to the base. An electrical resistance R represents the electrical circuit and Q denotes the electrical charge. The electromechanical coupling is provided by the piezoelectric element being represented by Ξ.

Therefore, the system dynamics may be described by the following equation

$$mz'' + bz' + kz - \frac{\Xi}{C}Q = -mu'' \tag{1}$$

$$RQ' - \frac{\Xi}{C}z + \frac{Q}{C} = 0 \tag{2}$$

where $(\blacksquare)' \equiv d(\blacksquare)/dt$.

The electromechanical coupling provided by the piezoelectric element, Ξ, needs to be properly described by some constitutive equation. The next section treats this modeling.

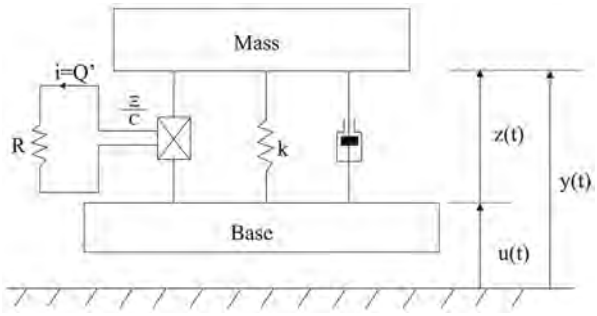

Figure 1. Archetypal model of the vibration-based energy harvesting system.
Source: Triplett and Quinn (2009).

Piezoelectric constitutive equations

The description of the three-dimensional (3D) behavior of the piezoelectric materials is now in focus. Hence, consider that S_i represent the strain, T_i represent the stress, D_i denote the electric displacement, and E_i the applied field. The elastic compliance, piezoelectric coupling, and permittivity matrices are denoted, respectively, by s_{ij}, d_{ij}, and ε_{ij}. The superscript "E" stands for measurements at zero or constant electric field, and "T" denotes measurements that are taken at zero or constant stress. Therefore, the 3D constitutive equations are given by

$$S_i = s_{ij}^E T_j + d_{mi} E_m \quad \text{(inverse effect)} \tag{3}$$

$$D_m = d_{mi} T_i + \varepsilon_{mk}^T E_k \quad \text{(direct effect)} \tag{4}$$

The inverse effect is associated with the generation of strain/stress in response to an applied electrical field, and the direct effect is related to electrical charge that is a response to an applied strain/stress. It is assumed that an axis-3 is associated with the poling direction, perpendicular to directions 1 and 2.

Some physical situations such as cantilever beams can be modeled as one-dimensional (1D) media, and therefore, the piezoelectric element can be designed to operate in either d_{31} or d_{33} mode of vibration depending on the arrangement of the electrodes. Figure 2(a) shows the d_{33} mode where stress is applied along axis-3 (in the direction of polarization), and the charge is collected in the same direction. The d_{31} mode, however, has stress applied along axis-1 (perpendicular to the direction of polarization), and charge is collected on the same surface as earlier (Figure 2(b)).

Coefficient d_{ij} establishes the relation between electric displacement and stress or strain and electric field. The linear model considers this piezoelectric coefficient as the slope of the linear fit of the strain–voltage curve

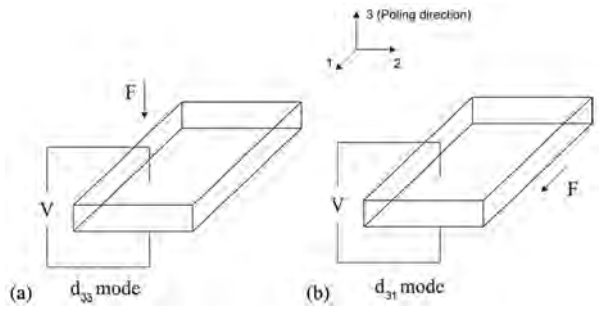

Figure 2. Operating mode of piezoelectric energy harvester transducer with axis-3 as a poling direction: (a) d_{33} mode and (b) d_{31} mode.

(Kang et al., 2011). Nevertheless, experimental data show that this electromechanical behavior is strongly dependent on the electric field intensity above certain threshold values, as shown in Figure 3(a), from experimental data of Crawley and Anderson (1990). From this curve, it is possible to use a secant method in order to determine the value of d_{31} as a function of strain (Figure 3(b)). Therefore, linear constitutive relation can be represented by a single constant value for all strain–electric fields (dashed curve in Figure 3(b)). A nonlinear approach of the piezoelectric coupling coefficient can be established by assuming a linear dependence on the induced strain, as proposed by Triplett and Quinn (2009) (dotted curve in Figure 3(b)).

Nonlinear approach for piezoelectric coupling coefficient proposed by Triplett and Quinn (2009) is described by the following equation

$$\Xi = \theta(1 + \beta|z|) \tag{5}$$

where θ and β are linear and nonlinear piezoelectric coupling coefficients, respectively. This approximation indicates that the coefficient can adopt different values depending on the induced strain.

Besides the nonlinear aspects presented in Figure 3, piezoelectric materials have a number of different nonlinear behaviors. Hysteretic behavior can be observed in the electric field–strain curves. Figure 4 presents the general electromechanical hysteretic behavior of piezoelectric materials, showing the following curves: strain–electrical field, d_{31}–electrical field, and d_{31}–strain. (Crawley and Anderson, 1990; Herdiera et al., 2007).

The hysteretic behavior of piezoelectric materials can be described by the Bouc–Wen model (Bouc, 1967), which has received an increasing interest due to its capability to capture a range of shapes of hysteretic cycles that match the behavior of a wide class of systems. In particular, it has been used to model piezoelectric elements. In our study, the Bouc–Wen model is employed to describe the strain-dependent hysteresis of the piezoelectric coupling, being represented by the following equations

$$\Xi = \Lambda(1 + \varrho|z| + \chi|\alpha|) \tag{6}$$

$$\alpha' = -\gamma|z'||\alpha|^{n-1}\alpha - \lambda z'|\alpha|^n + Az' \tag{7}$$

where $\Xi = \Xi(z, \alpha)$ represents the hysteretic piezoelectric coupling as the superposition of an elastic component $\Lambda(1 + \varrho|z|)$, similar to the nonlinear model, and a hysteretic component $\Lambda\chi|\alpha|$. The hysteretic behavior is described with the aid of a nondimensional variable α, and A, γ, λ, and n are nondimensional parameters, which control the shape and the size of the hysteresis loop. These parameters are adjusted in order to match experimental data of piezoelectric materials. This allows us to properly describe the electromechanical behavior of these materials. Several works discussed the physical meaning of these parameters (Ikhouane et al., 2007).

Equations of motion

Based on the discussion on constitutive models presented in the previous section, the energy harvesting system is now modeled. Therefore, piezoelectric constitutive equations are used together with the Bouc–Wen model in order to describe the hysteretic behavior of the piezoelectric element. Under these assumptions, the following equations of motion are adopted to describe the archetypal system presented in Figure 1

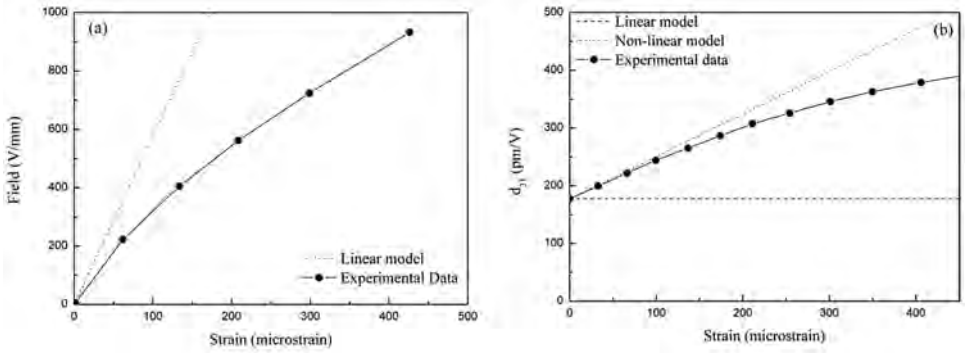

Figure 3. Electromechanical behavior of the piezoelectric materials: (a) electric field–strain curve and (b) d_{31}–strain curve.
Source: Crawley and Anderson (1990).

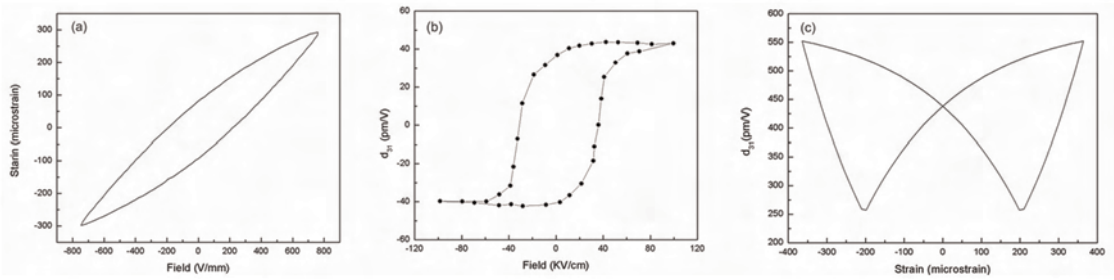

Figure 4. Electromechanical behavior of piezoelectric materials: (a) electric field–strain curve (Crawley and Anderson, 1990), (b) d_{31}–electrical field (Herdiera et al., 2007), and (c) d_{31}–strain curve derived from generic electric field–strain curve.

$$mz'' + bz' + kz - \frac{\Xi}{C}Q = -mu'' \tag{8}$$

$$RQ' - \frac{\Xi}{C}z + \frac{Q}{C} = 0 \tag{9}$$

$$\alpha' = -\gamma|z'||\alpha|^{n-1}\alpha - \lambda z'|\alpha|^n + Az' \tag{10}$$

$$\Xi = \Lambda(1 + \varrho|z| + \chi|\alpha|) \tag{11}$$

In order to obtain a nondimensional system, it is defined that coordinates $z = c_x x$ and $u = c_x v$, where c_x is a constant with dimension of inverse length. Moreover, it is assumed that $Q = c_q q$ and $\tau = \sqrt{k/m}t$, where c_q is a constant with dimension of inverse charge and $\sqrt{k/m}$ is a frequency Ω. Using $2\varsigma = b/m\Omega$ $\epsilon = c_q^2/c_x^2 m\Omega^2 C$, $\theta = (c_x/c_q)\Lambda$, $\rho = RC\Omega$, $\eta = c_x\varrho$, $\vartheta = c_x\Omega\gamma$, $\mu = c_x\Omega\lambda$, and $B = c_x\Omega A$. In these equations, $(\dot{\blacksquare})' \equiv d(\blacksquare)/d\tau$, where τ is the nondimensional time (Triplett and Quinn, 2009). The equations of motion are then rewritten as follows

$$\ddot{x} + 2\varsigma\dot{x} + x - \in \Theta q = \delta\sin\omega\tau - \phi \tag{12}$$

$$\rho\dot{q} - \Theta x + q = 0 \tag{13}$$

$$\dot{\alpha} = -\vartheta|\dot{x}||\alpha|^{n-1}\alpha - \mu\dot{x}|\alpha|^n + B\dot{x} \tag{14}$$

$$\Theta = \theta(1 + \eta|x| + \chi|\alpha|) \tag{15}$$

where $\delta\sin(\omega\tau - \phi)$ is a nondimensional excitation associated with base motion.

Numerical simulations are performed by employing the fourth-order Runge–Kutta method. In order to establish a comparison of the energy harvesting system dynamics, three different models for the piezoelectric electromechanical behavior are adopted: linear, nonlinear, and hysteretic. The instantaneous nondimensional electrical power is evaluated using the equation $P = \rho\dot{q}^2$.

Numerical simulations: linear and nonlinear models

This section discusses numerical simulations of the energy harvesting system establishing a comparison between linear and nonlinear models, following the same idea developed by Triplett and Quinn (2009). It should be highlighted that the coupling coefficient is assumed to be $\Theta = \theta(1 + \eta|x| + \chi|\alpha|)$, and the definition of the linear model assumes $\eta = 0$ and $\chi = 0$. This approach is valid for systems with small induced strains (Kim et al., 2010). Let us start the analysis by considering a linear model to describe piezoelectric coupling with $\delta = 2.0$, $\varsigma = 0.025$, $\rho = 1.0$, $\epsilon = 1.0$, and $\alpha = 0.0$. These parameters are based on the study by Triplett and Quinn (2009), which considers the equivalent nondimensional parameters obtained from experimental piezoelectric energy harvester developed by duToit and Wardle (2007). Figure 5(a) shows the results of average nondimensional power versus frequency. Figure 5(b) shows the results of the maximum nondimensional average power harvested as a function of linear piezoelectric coefficient. Note that there is an optimum value of θ close to 1.2.

The nonlinear model is now in focus by assuming the hysteretic coefficient $\chi = 0$ and different values for nonlinear coefficient η. The strain-dependent nonlinear model seems to be more appropriate to represent systems with large induced strains as pointed by Crawley and Anderson (1990). Figure 6(a) shows the results of the average nondimensional power versus frequency for $\theta = 1$ and different values of nonlinear coefficient η. Note that the increase in the nonlinear effect tends to shift maximum value of the power curve to the left. It is also noticeable that the maximum value changes, increasing and then decreasing. Figure 6(b) shows the results of maximum nondimensional average power harvested as a function of η or different values of linear coefficient θ.

Numerical simulations: hysteretic model

This section discusses the influence of the piezoelectric coupling hysteretic behavior on the energy harvesting system. Initially, we present quasi-static simulations that assume that the hysteresis loop of coupling coefficient is defined around average values defined from the nonlinear model (Triplett and Quinn, 2009). Quasi-static simulations are performed using equations (14) and (15) and assuming that a sinusoidal strain is prescribed, $z = \sin(\omega t)$, with $\omega = 2\pi$.

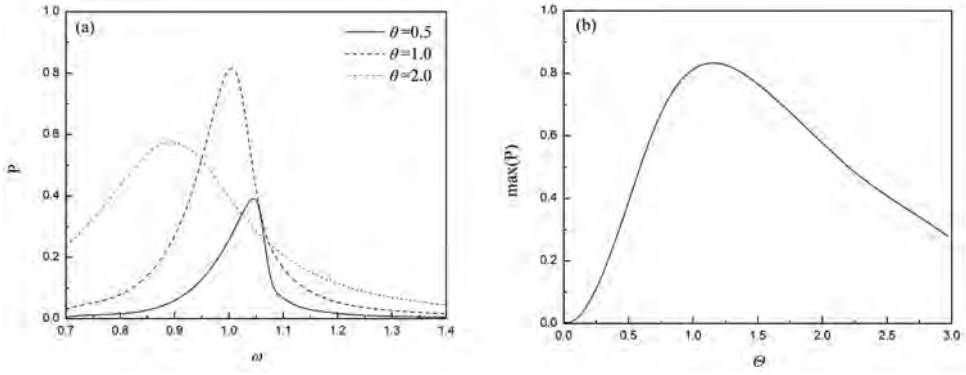

Figure 5. (a) Average nondimensional power harvested as a function of frequency for different values of linear piezoelectric coupling and (b) maximum nondimensional average power harvested as a function of linear piezoelectric coefficient.

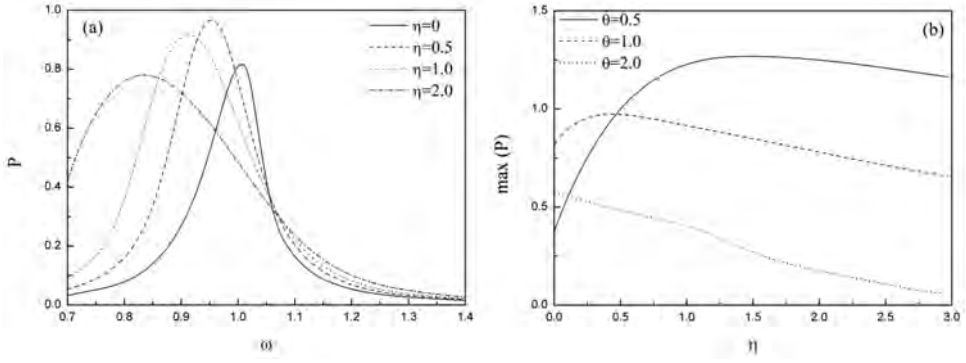

Figure 6. (a) Average nondimensional power harvested as a function of frequency for different values of nonlinear coefficient η (θ = 1) and (b) maximum nondimensional average power harvested as a function of nonlinear coefficient η for different values of θ.

Basically, three different average values of slopes are assumed as presented in Figure 7(a): 0.5, 1.0, and 2.0. All of them have approximately the same area. Besides, several hysteresis shapes are analyzed as shown in Figure 7(b), which illustrates this idea presenting cases around average value of 1.0. Three different situations related to hysteresis loop are considered: low, medium, and high hysteresis loop. These variations allow one to have a qualitative comprehension of the hysteresis loop influence, simulating different behaviors known as "hard" and "soft" piezoelectric transducer (PZT). In brief, soft PZT has higher piezoelectric constant, but larger losses in the material due to internal friction. Whereas hard PZT presents domain wall motion that is pinned by impurities, thereby lowering the losses in the material, but at the expense of a reduced piezoelectric constant (Stoleriu et al., 2010).

At this point, dynamical behavior of the energy harvesting system is analyzed using equations (12) to (15) under prescribed harmonic base excitation. Initially, dynamical evolution of the piezoelectric coupling behavior is investigated. The same three average values of slopes considered in the quasi-static analysis are considered (0.5, 1.0, and 2.0). Figure 8 presents the dynamic evolution of the piezoelectric coupling behavior Θ as a function of displacement, establishing a comparison with the nonlinear model. Note that the dynamic response evolves from the quasi-static configuration to a different one, with distinct average slope and area. When the average slope is 0.5 (Figure 8(a)), there is a considerable increase in the hysteresis area when compared with the quasi-static behavior (Figure 7(a)). Moreover, the average slope decreases, and the value of the piezoelectric coupling at $x = 0$ moves for larger values from the initial position to the steady state. This effect becomes smaller when the initial average value increases and almost disappears when the average slope is 2.0 (Figure 8(c)). Another aspect that should be pointed out is that initially, the wing curve format has an asymmetric aspect, tending to become symmetric in the steady-state response. This behavior can be explained by observing the displacement time history. Let us consider the sets of parameters related to Figure 8 for this aim. The displacement time history for these systems are presented in Figure 9 that shows a transient response related to changes in hysteretic

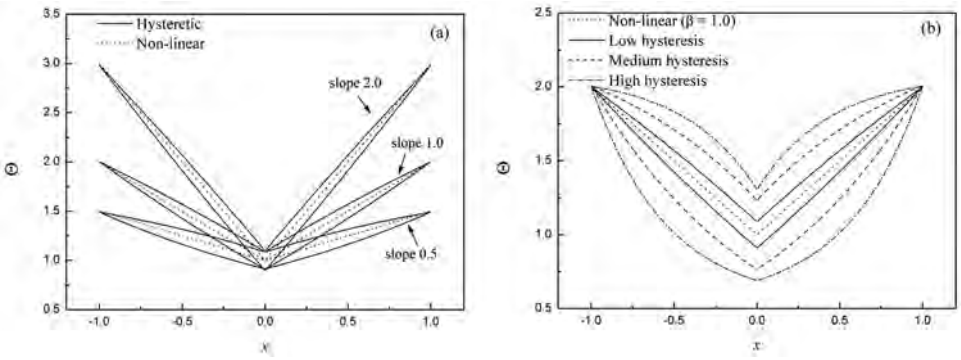

Figure 7. (a) Quasi-static $\Theta(x, \alpha)$ as a function of strain around three different average values of slopes and (b) three different quasi-static $\Theta(x, \alpha)$ as a function of strain around average value of 1.0.

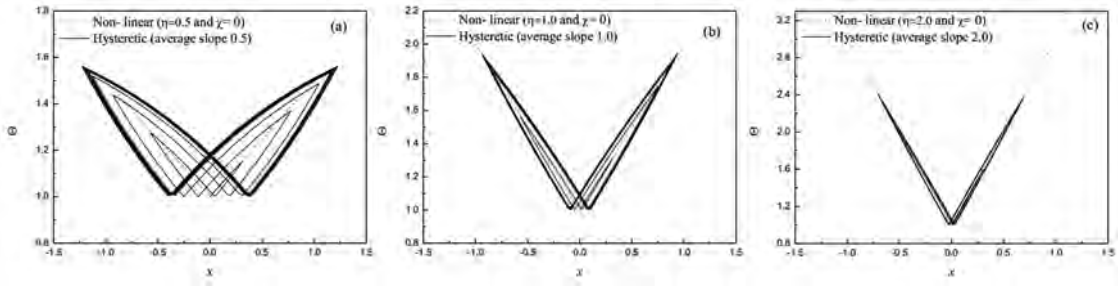

Figure 8. Three different dynamic behaviors of the piezoelectric coupling $\Theta(x, \alpha)$ as a function of displacement around one average value of slope of (a) 0.5, (b) 1.0, and (c) 2.0 ($\omega = 1$ and $T = 2\pi$).

behavior, and a steady-state response, associated with a symmetric hysteretic wing.

The forthcoming analysis is related to the nondimensional average power generated in the energy harvesting system. Essentially, different frequency excitations are considered evaluating the general behavior of the system. Once again, different hysteretic behaviors are of concern, establishing a comparison with linear and nonlinear models. Figure 10 shows the average power as a function of frequency for three different average slopes of the piezoelectric coupling behavior shown in Figure 8. When compared with the linear model, both nonlinear and hysteretic models have similar behaviors. As the average slope of the piezoelectric coupling increases, the maximum power frequency presents a shift to the left. Their maximum values initially increase and then decrease. Now, when comparing results of the nonlinear model with those of the hysteretic models, it is possible to see that the maximum power is always greater for the hysteretic case, and these maxima increase as the average slope decreases.

Now, we want to investigate the influence of the hysteresis loop area on the energy harvesting power. Figure 11 presents the dynamic behavior of the piezoelectric coupling Θ as a function of displacement around a slope value of 1.0 but with different hysteresis area, as shown in the quasi-static analysis (Figure 7(b)). The same effects observed in Figure 8 can be observed here: the average slope decreases from the initial state to the steady state. Moreover, the value of the piezoelectric coupling at $x = 0$ moves for larger values, and these effects become increasingly greater with the increase in the hysteresis.

Figure 12 shows the average power as a function of frequency for these three hysteretic piezoelectric couplings shown in Figure 11. Note that the power increases and then decreases slightly when hysteretic behavior increases. Besides, there is a movement of the peak values for high frequencies in comparison with nonlinear model. As expected, low hysteretic behavior presents responses close to the nonlinear model.

The general tendency of the maximum value of the generated average power is summarized in Figure 13. Linear, nonlinear, and hysteretic results are plotted together versus different levels of hysteresis. Therefore, since linear and nonlinear models do not present hysteresis, they have constant values for all simulations. These values are plotted in the first position of the horizontal axis. The slope of the nonlinear model and the hysteresis loop area establish a competition that can cause the increase or the decrease in the maximum power value. The maximum of the average power initially increases and then decreases with the increase in the hysteresis loop area of the piezoelectric coupling.

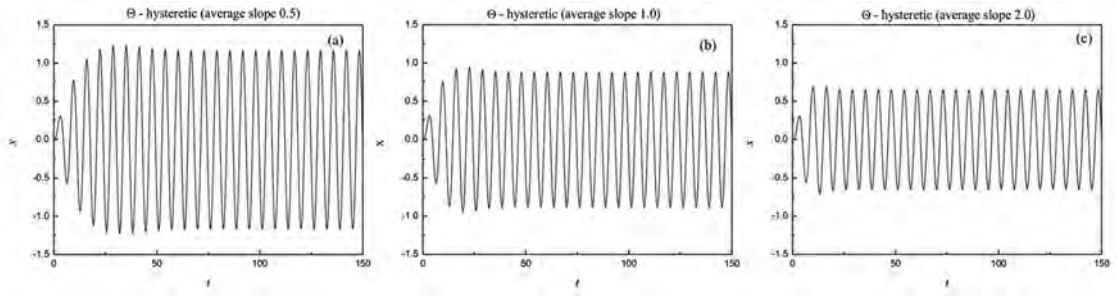

Figure 9. Displacement time history for the cases shown in Figure 8: (a) average value of slope of 0.5, (b) average value of slope of 1.0, and (c) average value of slope of 2.0.

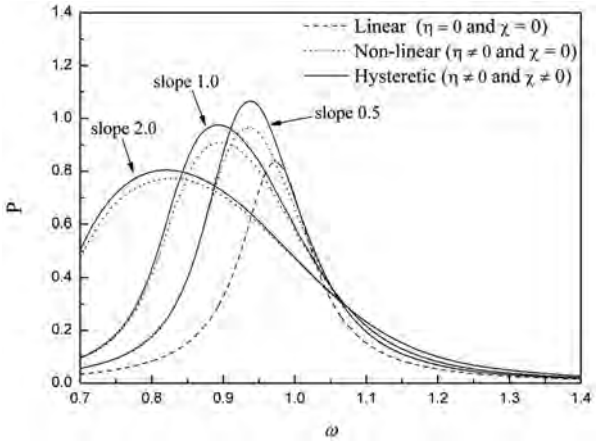

Figure 10. Average nondimensional power versus frequency: comparison among linear, nonlinear, and hysteretic models for three different average values of slopes.

These results suggest that there is an optimum hysteretic behavior that increases the power output of the energy harvester.

Conclusion

This article deals with the influence of the hysteretic behavior of the piezoelectric element on vibration-based energy harvesting systems. The Bouc–Wen model is employed to describe the electromechanical hysteretic behavior of the piezoelectric element. Numerical simulations are carried out considering different hysteretic behaviors showing their influence on system dynamics. Results of the hysteretic system are compared with those obtained for nonlinear and linear piezoelectric behaviors. The average slope of the hysteresis and the hysteresis level of piezoelectric coupling establish a competition to define the generated power. Results show that piezoelectric hysteretic nonlinearity can significantly influence the performance of the system in terms of the harvested power. Moreover, it is important to observe that results suggest that there is an optimum hysteretic behavior that increases the power output of the energy harvesters.

Acknowledgements

The authors would like to thank the Brazilian Research Agencies CNPq, CAPES, and FAPERJ, and through the INCT-EIE (National Institute of Science and Technology—Smart Structures in Engineering), the CNPq and FAPEMIG for their support. The Air Force Office of Scientific Research (AFOSR) is also acknowledged.

Funding

This research received the following specific grant numbers: FAPERJ E26/102.306/2009 and FAPERJ E26/102.830/2012 CNPq 300.723/2009-1 and CNPq 574.001/2008-5 AFOSR FA9550-11-1-0284.

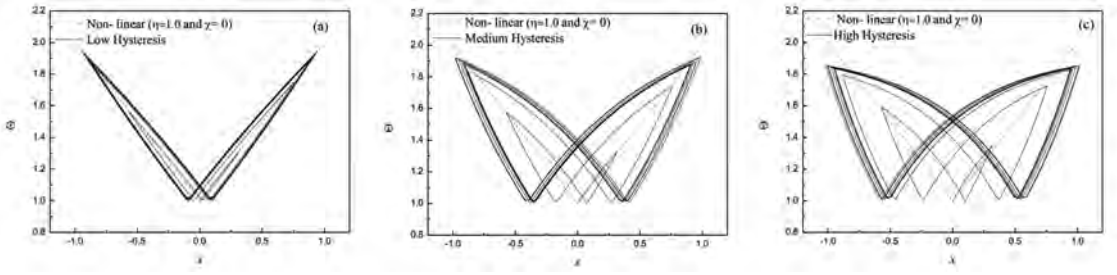

Figure 11. (a–c) Three different dynamic behaviors of the piezoelectric coupling $\Theta(x, \alpha)$ as a function of displacement around one average value of slope of 1.0 ($\omega = 1$ and $T = 2\pi$).

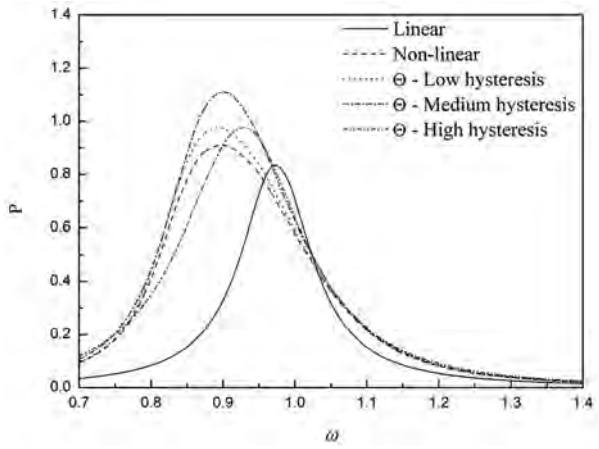

Figure 12. Average nondimensional power versus frequency. Hysteretic piezoelectric coupling around an average value of slope of 1.0, with three different hysteresis levels.

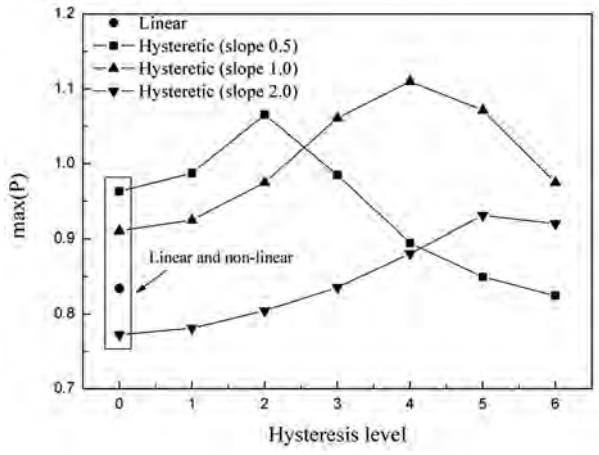

Figure 13. Comparison between maximum values of the nondimensional power harvested.

References

Bouc R (1967) Forced vibration of mechanical systems with hysteresis. In: *Proceedings of the fourth conference on nonlinear oscillation*, Prague, Czech Republic, p. 315, 5–9 September 1967.

Crawley EF and Anderson EH (1990) Detailed models of piezoceramic actuation of beams. *Journal of Intelligent Material Systems and Structures* 1: 4–25.

Crawley EF and de Luis J (1987) Use of piezoelectric actuators as elements of intelligent structures. *AIAA Journal* 25(10): 1373–1385.

duToit NE and Wardle BL (2006) Performance of microfabricated piezoelectric vibration energy harvesters. *Integrated Ferroelectrics* 83: 13–32.

duToit NE and Wardle BL (2007) Experimental verification of models for microfabricated piezoelectric vibration energy harvesters. *AIAA Journal* 45: 1126–1137.

Erturk A and Inman DJ (2011) *Piezoelectric Energy Harvesting*. Chichester: John Wiley & Sons Ltd.

Herdiera R, Jenkins D, Remiens D, et al. (2007) A silicon cantilever beam structure for the evaluation of d_{31}, d_{33} and e_{31} piezoelectric coefficients of PZT thin films. In: *16th IEEE international symposium on applications of ferroelectrics*, pp. 725–727, 27–31 May 2007, Nara-City, Japan.

Hu YR and Ng A (2005) Active robust vibration control of flexible structures. *Journal of Sound and Vibration* 288(1–2): 43–56.

Ikhouane F, Mañosa V and Rodellar J (2007) Dynamic properties of the hysteretic Bouc-Wen model. *Systems & Control Letters* 56: 197–205.

Kang LH, Lee DO and Han JH (2011) A measurement method for piezoelectric material properties under longitudinal compressive stress a compression test method for thin piezoelectric materials. *Measurement Science and Technology* 22: 065701.

Kim M, Hoegen M, Dugundji J, et al. (2010) Modeling and experimental verification of proof mass effects on vibration energy harvester performance. *Smart Materials and Structures* 19: 045023.

Liao WH, Wang DH and Huang SL (2001) Wireless monitoring of cable tension of cable-stayed bridges using PVDF piezoelectric films. *Journal of Intelligent Material Systems and Structures* 12: 331–339.

Roundy S, Steingart D, Frechette L, et al. (2004) Power sources for wireless sensor networks. *Lecture Notes in Computer Science* 2920: 1–17.

Sodano HA, Inman DJ and Park G (2004) A review of power harvesting from vibration using piezoelectric materials. *The Shock and Vibration Digest* 36(3): 197–205.

Stoleriu L, Ciomaga1 C, Fochi F, et al. (2010) Mechanically clamped PZT ceramics investigated by first-order reversal curves diagram. *Processing and Application of Ceramics* 4(3): 209–214.

Triplett A and Quinn DD (2009) The effect of non-linear piezoelectric coupling on vibration-based energy harvesting. *Journal of Intelligent Material Systems and Structures* 20: 1959–1967.